HHS Public Access

Author manuscript

J Invest Dermatol. Author manuscript; available in PMC 2016 January 20.

Published in final edited form as:

J Invest Dermatol. 2015 July ; 135(7): 1820–1828. doi:10.1038/jid.2015.61.

Genome-wide DNA methylation analysis in melanoma reveals the importance of CpG methylation in *MITF* regulation

Martin Lauss[1,2], **Rizwan Haq**[3], **Helena Cirenajwis**[1,2], **Bengt Phung**[1], **Katja Harbst**[1,2], **Johan Staaf**[1,2], **Frida Rosengren**[1], **Karolina Holm**[1,2], **Mattias Aine**[1], **Karin Jirström**[1,4], **Åke Borg**[1,2], **Christian Busch**[5], **Jürgen Geisler**[6,7], **Per Eystein Lønning**[5], **Markus Ringnér**[1,2], **Jillian Howlin**[1], **David Fisher**[3], and **Göran Jönsson**[1,2]

[1]Division of Oncology and Pathology, Department of Clinical Sciences, Lund University, Lund, Sweden

[2]CREATE Health Strategic Center for Translational Cancer Research, Lund University, Lund, Sweden

[3]Departments of Dermatology and Medical Oncology, Massachusetts General Hospital, Boston, USA

[4]Department of Clinical Pathology, Skåne University Hospital, Lund, Sweden

[5]Section of Oncology, Institute of Medicine, University of Bergen, Bergen, Norway

[6]Department of Clinical Molecular Biology and Laboratory Sciences, Akershus University Hospital, Lørenskog, Norway

[7]Institute of Clinical Medicine, University of Oslo, Oslo, Norway

Abstract

The microphthalmia-associated transcription factor (MITF) is a key regulator of melanocyte development and a lineage-specific oncogene in melanoma; a highly lethal cancer known for its unpredictable clinical course. MITF is regulated by multiple intracellular signaling pathways although the exact mechanisms that determine MITF expression and activity remain incompletely understood. In this study, we obtained genome-wide DNA methylation profiles from 50 stage IV melanomas, normal melanocytes, keratinocytes and dermal fibroblasts, and utilized The Cancer Genome Atlas (TCGA) data for experimental validation. By integrating DNA methylation and gene expression data we found that hypermethylation of *MITF* and its co-regulated differentiation pathway genes, corresponded to decreased gene expression levels. In cell lines with a hypermethylated MITF-pathway, over-expression of MITF did not alter the expression level or methylation status of the MITF pathway genes. In contrast however, demethylation treatment of these cell lines induced MITF-pathway activity, confirming that gene-regulation was controlled via methylation. The discovery that the activity of the master regulator of pigmentation, *MITF*, and its downstream targets may be regulated by hypermethylation has significant implications for understanding the development and evolvement of melanoma.

Corresponding author: Göran Jönsson, Department of Oncology and Pathology, Clinical Sciences, Medicon Village, Scheelevägen 2, Lund University, Lund, 223 81, Sweden. Phone: +46 46 2221444. Goran_B.Jonsson@med.lu.se.

Disclaimers: No disclosures

Keywords

Melanoma; MITF; DNA methylation; gene expression; melanocytes; Polycomb

Introduction

Tumorigenesis is accompanied by diverse genomic and epigenomic alterations, including somatic mutations, copy number variations (CNVs) and changes in DNA methylation patterns. The significance of somatic mutations and CNVs has been investigated in melanoma, highlighting the pattern of UV-induced mutations (Hodis *et al.*, 2012; Krauthammer *et al.*, 2012). Specifically, early mutation screening studies identified *BRAF* mutations in a significant fraction of melanoma tumors (Davies *et al.*, 2002). These findings subsequently led to the development of targeted therapies directed towards *BRAFV600E* mutated cells (Chapman *et al.*, 2011; Davies *et al.*, 2002).

Melanomas originate from melanocytes that are melanin-producing cells. While the bHLHZip microphthalmia-associated transcription factor (MITF) is the master regulator of melanin-production (pigmentation) (Steingrimsson *et al.*, 2004) early studies also identified *MITF* as a lineage-specific oncogene in melanoma and found that amplification of *MITF* was associated with inferior survival (Garraway *et al.*, 2005). Additionally, rare variants of the *MITF* gene predispose to melanoma (Yokoyama *et al.*, 2011). Collectively, these observations support the idea of a tight connection between melanocyte differentiation and melanoma initiation and progression. We have previously shown that melanoma can be subdivided into at least four gene-expression phenotypes; one of these phenotypes is characterized by increased *MITF* expression and another by high expression of proliferation-associated genes coupled with decreased expression of *MITF* and its downstream targets (Harbst *et al.*, 2012; Jonsson *et al.*, 2010).

In melanoma, the epigenetic landscape has been previously investigated and a subset of melanomas with increased CpG island methylation levels, similar to findings from other cancer forms, has been described. This melanoma phenotype has been termed the CpG Island Methylator Phenotype (CIMP) (Noushmehr *et al.*, 2010; Tanemura *et al.*, 2009; Weisenberger *et al.*, 2006). Conversely, a small number of genes have shown to be hypomethylated, and thereby activated, in melanoma (van den Hurk *et al.*, 2012). High-throughput technology has enabled the screening for biomarkers that discriminate melanoma from nevi or melanocytes (Bonazzi *et al.*, 2011; Conway *et al.*, 2011; Furuta *et al.*, 2006; Gao *et al.*, 2013; Gao *et al.*, 2014; Koga *et al.*, 2009; Li *et al.*, 2013), the discovery of methylation subgroups (Sigalotti *et al.*, 2012; Thomas *et al.*, 2014) as well as more dedicated studies (Dahl *et al.*, 2014; Ecsedi *et al.*, 2014; Lian *et al.*, 2012; Marzese *et al.*, 2013; Marzese *et al.*, 2014).

To further define genes whose expression is regulated by DNA methylation in melanomas, we have comprehensively investigated the epigenetic landscape of melanoma using high-density genome-wide CpG microarrays. Integrating DNA methylation and gene expression data highlighted the *MITF* gene since tumors with decreased *MITF* expression also displayed hypermethylated MITF-associated CpGs. Importantly, these CpGs were located at

the transcription start site (TSS) of the melanocyte-specific transcript MITF-M. Our findings reveal the regulation of the MITF pathway by CpG hypermethylation and highlight the potential significance of epigenetic changes in melanoma tumorigenesis

Results

DNA methylation patterns in melanoma tumors

We herein describe the epigenetic landscape of melanoma by analysis of the DNA methylation status of more than 480,000 CpGs in 50 metastatic melanoma tumors (Bergen melanomas). To determine the DNA methylation status specific to melanoma cells, we measured the DNA methylation in both cultured melanocytes (light, medium and dark melanocytes) and tumors. We defined melanoma-methylated CpGs as $\beta<0.1$ in melanocytes and $\beta>0.5$ in at least 20% of tumors; and melanoma-hypomethylated CpGs as $\beta>0.9$ in melanocytes and $\beta<0.5$ in at least 20% of tumors. A larger fraction of CpGs was methylated (n=9,886) rather than hypomethylated (n=5,236) in melanomas.

Hypomethylated CpGs were preferentially located in intergenic regions and gene bodies and in the 'open sea' (located away from CpG islands). In contrast, hypermethylated CpGs were preferentially located in CpG islands (Figure 1A). Tumors, in general, had low DNA methylation levels near the TSS and high methylation levels in gene bodies, 3'UTRs, and intergenic regions (Figure 1B). The variation in β-values was considerably lower for CpGs within 200 bp upstream of the TSS and for 3'UTRs (Figure 1B). Hence, CpGs upstream of the TSS were predominantly hypomethylated whereas CpGs in 3'UTRs were predominantly hypermethylated. GO term analysis of hypomethylated CpG associated genes using DAVID (Huang da *et al.*, 2009) showed enrichment of genes situated in the plasma membrane ($FDR=1\times10^{-21}$) and involved in system development ($FDR=8\times10^{-12}$). The hypermethylated CpGs in contrast were overrepresented in genes that regulate cell differentiation ($FDR=3\times10^{-46}$) as well as genes with a Homeobox domain ($FDR=1\times10^{-31}$). Furthermore, there was a strong preference for developmental genes ($p=2\times10^{-73}$) and embryonic stem cell-derived PRC2 targets ($p=1\times10^{-216}$) to be methylated in melanomas (Figure 1A). PRC2 is a complex with histone methyltransferase activity and DNA hypermethylation of its target genes in embryonic stem cells is in agreement with findings in other tumor types (Easwaran *et al.*, 2012).

To further validate these findings, we compared our results with the DNA methylation status of 244 melanomas from The Cancer Genome Atlas (TCGA) project (https://tcga-data.nci.nih.gov/tcga/). Using the same analysis procedure we found 5,752 hypomethylated CpGs and 10,426 hypermethylated CpGs that were identical to 76% and 90% of Bergen CpGs, respectively. Our findings indicate that aberrant DNA methylation events in melanomas are reproducible and in particular a strong preference for hypermethylation of developmental genes/PRC2-target genes is observed.

MITF expression is regulated by DNA methylation

The proliferative gene expression phenotype is characterized by down-regulation of immune response and pigment synthesis genes (Jonsson *et al.*, 2010). However, the biological

mechanism underlying the expression signature is not fully investigated. Thus, we aimed to explore DNA methylation events that correlated with gene expression in melanoma. We used tumor cohorts with matching genome-wide methylation and gene expression data to allow us to identify genes whose expression is primarily regulated by DNA methylation. We found 2,922 negatively correlated CpGs (Spearman correlation<−0.39) and 2,406 positively correlated CpGs (correlation>0.39) (FDR<0.05), corresponding to 1,119 and 503 unique genes, respectively (Table S1). Negative correlation was preferentially observed for CpGs within 200bp upstream of TSS and positive correlation for CpGs within gene bodies (Figure S1). GO terms were not identified for either positively or negatively correlated CpGs at FDR<0.01. Notably, among the genes with a negative correlation between methylation and gene expression, *MITF* was highly ranked, having the 44th most negative correlation genome-wide. The DNA methylation status of six CpGs associated with the *MITF* gene was coupled to reduced *MITF* expression in the Bergen cohort. As expected, the DNA methylations status of these *MITF* CpGs was associated with gene expression phenotypes when using an average β-value across these six CpGs (*P*=0.0003, Kruskal-Wallis test). Typically, melanomas of the pigmentation gene expression phenotype had low methylation levels coupled with high expression levels of *MITF*, whereas melanomas of the proliferative phenotype displayed the opposite pattern: high methylation levels associated with low gene expression levels (Figure 2A). In total, 49 CpGs covering the *MITF* gene were present on the array. Of the six CpGs that were significantly negatively associated with gene expression levels of *MITF*, three were located at the TSS of the M-isoform of *MITF* (the active isoform in melanocytes and melanoma cells) while three were located within the body of the *MITF-M* transcript close to the TSS (Figure 2A). A detailed analysis of the CpGs covering *MITF* demonstrated that the majority of CpGs showed limited variation in methylation across tumors with the exception of the CpGs located close to the *MITF-M* TSS. Specifically, CpGs located within the body of the *MITF* gene were hypermethylated and all CpGs located at the TSS of the long isoform were hypomethylated across all tumors and normal cells (Figure 3). Furthermore, genome-wide CpG analysis of three melanocyte strains, dermal fibroblast, keratinocytes and lymphocytes showed similarly consistent results. In normal melanocytes, the six CpGs located near the *MITF-M* TSS were all hypomethylated, while in all other normal cells they were hypermethylated (Figure 3). Subtle differences in methylation values were observed in the cultured melanocytes with highest methylation values in the light melanocytes and lowest in the dark melanocytes. However, it should be noted that all three strains had very low β-values corresponding to hypomethylation (Figure 3). Further analysis of the negatively associated list of CpGs demonstrated that some of these were located at the TSS of well-known MITF target genes involved in pigment synthesis such as *MLANA* and *TYR* (Figure 3). *MLANA* and *TYR* showed the same pattern as *MITF*: tumors with low expression and DNA hypermethylation of the respective genes were typically of the proliferative phenotype (Figure 2B–C). Overall, the majority of correlated CpGs, including the CpGs of *MITF* and MITF target genes (Cheli *et al.*, 2010)) identified in the Bergen cohort were validated in the TCGA cohort as shown in Figure 4. CpGs located at the TSS of *MLANA* and *TYR* correlated with gene expression, while the non-correlated CpG within the gene body of *TYR* displayed hypermethylation across all tumors as well as normal cells (Figure 3). Moreover, MITF target genes unrelated to pigmentation, such as *BCL2* and

RAB27A, tended to show hypermethylation near the TSS in tumor samples with low mRNA levels of *MITF* (Figure 3).

MITF pathway hypermethylation in melanoma cell lines

Next, we investigated genome-wide DNA methylation status of nine melanoma cell lines to determine if the MITF pathway hypermethylation is independent of the melanoma tumor microenvironment. DNA methylation and gene expression correlation values in the cell line data showed an overlap of significantly correlated CpGs. Importantly, correlations of CpGs belonging to *MITF*, MITF targets, and MITF pathway genes were readily confirmed (Figure 5A). The *MITF* high-expressing cell line SK-MEL-5 showed hypomethylation of the identified *MITF-M* CpGs and CpGs in well-known targets of MITF such as *TYR* and *MLANA*. Conversely, the 'MITF-low' cell lines CHL1, WM852 and MM383 showed hypermethylation of these same CpGs, supporting the results obtained from the tumor cohorts (Figure 5B). Investigating mRNA levels of the selected MITF target genes (*MITF*, *MLANA*, *TYR*, *BCL2*, *RAB27A*) across the cell lines, we found that these overall followed the DNA methylation patterns (Figure 5C). Moreover, immunohistochemistry revealed that the cell lines, A2058 and HT144, with intermediate *MITF* expression consisted of both *MITF* positive and *MITF* negative cells (Figure 5D). As methylation levels of some CpGs tended to be intermediate in these cells, this suggests that some cells are hypomethylated and some are fully methylated. Finally, we validated the *MITF* hypermethylation observed in the melanoma cell lines using bisulphite Sanger sequencing (Figure 5B). Together, this implies that the observed link between DNA methylation and *MITF* expression is not dependent on the tumor microenvironment, but instead is established within the tumor cells.

MITF is not sufficient to modulate DNA hypermethylation in melanoma

To investigate the nature of the relationship between *MITF* expression and DNA methylation, we overexpressed *MITF-M* in 'MITF-low' cell lines (WM852 and MM383) using a lentivirus system. These cell lines were selected based on low levels of *MITF* mRNA and hypermethylation of CpGs located at the TSS of *MITF-M* and MITF target genes (Figure 5B). Ten days after infection, we confirmed overexpression of the MITF protein (Figure 6C). We also analyzed the *MITF-M* overexpressing cells using the 450K-methylation arrays. The candidate MITF target and pathway CpGs remained firmly methylated. We then selected MLANA as a well-known MITF target previously shown to be activated by inducing MITF (Du *et al.*, 2003), and investigated *MLANA* mRNA and protein levels (Figure 5C, 6E). As indicated by the DNA methylation analysis, no increase in MLANA protein levels was seen suggesting that *MITF-M* alone is not sufficient to shift the epigenetic program of the MITF differentiation pathway genes (Figure S2). This hypothesis was further supported by gene expression analysis demonstrating that there is almost no change in expression of the MITF target genes in these cells (Figure 5C).

Global demethylation treatment reactivates MITF pathway activity

To evaluate if DNA methylation blocks *MITF* expression in the 'MITF-low' cell lines, we induced global demethylation of the cell lines by 5'-Aza-2'-Deoxycytidine (5-Aza) treatment for 96 hours. Demethylation was confirmed by bisulphite Sanger sequencing

(Figure 6A). In particular, the cytosine to thymidine ratio decreased when treating cells with 5-Aza indicating that demethylation had occurred. Furthermore, the demethylation treatment was sufficient to restore MITF protein levels in both cell lines (Figure 6B). Moreover, the viability of melanoma cells treated with 5-Aza alone was significantly decreased only after 96 hours in both cell lines ($P<0.001$, Mann-Whitney Test), while the invasive capacity of the cells was not altered ($P>0.05$, Mann-Whitney Test) (Figure 6C and D). The late effect on cell viability could suggest that there is a non-specific toxic effect of 5-Aza. Furthermore, we found no effect of single agent BRAF inhibition in the BRAF V600E positive 'MITF-low' MM383 cell line on viability. Combining 5-Aza and PLX4032 showed a slight additive effect on viability at 96 hours as compared to either 5-Aza or PLX4032 alone ($P<0.01$, Mann-Whitney Test, Figure 6D).

To further investigate the effect of MITF induction by 5-Aza we analyzed the levels of MLANA. No induction of MLANA levels was observed, suggesting that the 5-Aza induces MITF-M expression but not MITF-M activity (Figure 6E). To further establish that the downstream targets of MITF are also regulated by methylation events, we treated the *MITF-M* over-expressing MM383 and WM852 cells with 5-Aza because these cells would have abundant exogenous MITF-M to induce MITF target expression if these were regulated by DNA methylation. Demethylation was confirmed by bisulphite Sanger sequencing (Figure 6F). We observed a slight increase in MITF-M levels, which was accompanied by restoration of MLANA protein levels (Figure 6E). It should be noted that MLANA expression is only partially induced by the exogenous MITF-M. This is demonstrated by the relatively low MLANA expression as compared to MLANA levels in SK-MEL-3 even though only a fifth of the total amount of SK-MEL-3 protein as compared to the other samples was loaded on the gel (Figure 6E). Thus, following MITF-over-expression and demethylation treatment, some functional MITF is produced, albeit at a low level, and can induce low levels of MLANA.

Discussion

In the current study, we have compared genome-wide DNA methylation profiles from melanoma tumors with normal melanocytes. The analysis highlighted preferential hypermethylation of genes belonging to developmental processes and PRC2 complex targets; a finding previously demonstrated in multiple cancer types (Easwaran *et al.*, 2012). Interestingly, combining gene expression and DNA methylation data revealed that a number of genes involved in pigment synthesis were regulated by hypermethylation, including *MITF* and several well-known MITF target genes. MITF is a master regulator of melanocyte differentiation (Steingrimsson *et al.*, 2004) and the *MITF-M* isoform has been shown to function as a lineage-specific oncogene, with amplification occurring in approximately 10% of melanomas (Garraway *et al.*, 2005; Jonsson *et al.*, 2007). Moreover, studies have shown that genes involved in developmental processes are kept in relatively stable 'on' or 'off' states, with tumor specimens across many cancer types having enforced the 'off' state by DNA methylation (Easwaran *et al.*, 2012). Our data suggest that key melanocyte genes, such as *MITF*, are regulated in such a way. Melanocytes are *MITF*-'on' cells, and it is possible that *MITF*-'off' clones are generated during tumor evolution. Methylation events during tumor evolution often occur over many cell divisions and have a stochastic component

(Landan *et al.*, 2012) with different epigenetic states leading to diverging tumor cell subpopulations (Sharma *et al.*, 2010). Hence, it is conceivable that subpopulations of melanoma cells emerge that have lost all MITF-positive cells and are therefore 'locked' to the MITF-'off' state. Importantly, a demethylation agent re-induced MITF-M expression in 'MITF-low' cell lines, indicating that demethylation is one of the factors required to rescue MITF-M expression. Treating 'MITF-low' cell lines that exogenously overexpressed *MITF-M* with a demethylating agent, led to partial induction of MLANA, a downstream target of MITF. The lack of strong MLANA induction, despite high expression of MITF, is consistent with the possibility that post-translational modification of MITF is necessary for its activity as previously described (Mansky *et al.*, 2002; Miller *et al.*, 2005; Murakami and Arnheiter, 2005; Vashisht Gopal *et al.*, 2014; Wu *et al.*, 2000; Yokoyama *et al.*, 2011). Furthermore, these results also indicate that intrinsically 'MITF-low' melanoma cells may be programmed to inactivate MITF-M by post-translational modifications and that over-expression of exogenous *MITF-M* saturates the post-translational inactivation mechanisms, thus requiring abundant MITF-M in combination with 5-Aza to activate downstream targets. Although, further studies are warranted to determine the post-translational modification state of MITF, our study provide evidence showing that *MITF-M* expression and activity can be regulated by DNA methylation. Importantly, we previously identified a gene expression phenotype with decreased mRNA levels of *MITF* and MITF target genes and herein we conclude that this phenotype may partially be explained by hypermethylation events. In a recent study, Konieczkowski et al. found that 'MITF-low' melanoma cells are intrinsically resistant to MAPK inhibitors (Konieczkowski *et al.*, 2014). Thus, it is intriguing to speculate that hypermethylation of the MITF pathway may be a marker of resistance to MAPK inhibition. Indeed, we showed that the BRAF V600E positive MM383 melanoma cell line harboring *MITF-M* promoter methylation did not respond to BRAF inhibition. Furthermore, we also tested the effects of 5-Aza on melanoma cell viability and invasion. Although, 5-Aza decreased viability and did not significantly affect invasion this could be explained by the non-specific toxic activity of 5-Aza. Due to the complexity of regulation of MITF activity in melanoma cells, further studies are required to understand the mechanism of demethylating agents in melanoma.

In summary, we found that the activity of the master regulator of pigmentation, MITF, may be regulated by hypermethylation and this is of fundamental importance for the understanding of the development and evolvement of melanoma.

Material and Methods

Tumor and cell line cohorts analyzed for methylation patterns

We performed genome-wide methylation analysis using the Illumina Infinium HumanMethylation450K BeadChip in 50 stage III/IV tumors (Table S2), nine melanoma cell lines, light, medium, and dark melanocytes, dermal epidermis, fibroblasts (Science Cell Research), and peripheral blood leukocytes (Promega) (Supplementary methods). Written informed consent was obtained from all patients and the local ethics committee approved the study. DNA was extracted as previously described (Jonsson *et al.*, 2010) and was bisulphite treated using the EZ DNA Methylation Kit (Zymo) according to manufacturer's instructions.

Methylation and gene expression data is available as Gene Expression Omnibus series GSE51547 and GSE22153, respectively.

Correlation of gene expression and methylation data

For methylation/gene expression correlation analyses CpGs with methylation levels having standard deviation < 0.2 across tumors were excluded. The remaining features were permuted to obtain a data driven false discovery rate. This filter is advisable, as slight technical variation of β-values can be introduced by copy number aberrations, which in turn are correlated with gene expression (Lauss *et al.*, 2012). The matched gene expression data were processed as previously described (Jonsson *et al.*, 2010), multiple probes of a gene were median-merged, and the 50% most varying genes were kept. Detailed analysis procedures for the different data sets are described in supplementary information.

Bisulphite Sanger sequencing, immunohistochemistry and western blots

MITF-M was over-expressed using a lentivirus system as previously described (Haq *et al.*, 2013). Western blot was performed with antibodies against MITF-M (C5, Thermo Scientific) and MLANA (EP1422Y, Abcam). DNA primers were designed to specifically amplify bisulphite converted genomic DNA of a distinct region covering the *MITF* promoter including CpGs covered by the array. The sequencing products were sequenced using a 3130XL sequencer. For MITF-M immunohistochemical analysis, 2 mm sections were automatically pre-treated using the PT-link system (DAKO, Glostrup, Denmark) and stained in an Autostainer Plus (DAKO,) using a monoclonal MITF-antibody (C5, Thermo Scientific, diluted 1:50).

5-Aza treatment, cell viability and invasion assays

MM383 and WM852 cells were seeded at a density of 9×10^3 cells/cm^2 treated 24 hours later with 5μM 5-Aza. The drug was replenished every 24 hours for up to 96 hours of treatment (4 pulses) in fresh medium. DNA, RNA and protein were isolated for molecular analyses. Cell viability was measured using an AlamarBlue assay and migration/invasion using the real time cell analyzer (RTCA) xCELLigence system (ACEA Biosciences). For the AlamarBlue assay, cells were seeded at a density of 12×10^3 cells/cm^2 (4000 cells/well) in 21 replicates per treatment. Cells were treated with 5-Aza (5μM), PLX4032 (200nM) or 5-Aza (5μM) + PLX4032 (200nM) 24 hours after seeding. The drugs were replenished every 24 hours for up to 96 hours of treatment (4 pulses) in fresh medium. Statistics were performed using the Mann–Whitney U test.

For the invasion experiments, melanoma cells were serum starved prior to cell seeding. Cells were seeded into the upper chamber of the invasion CIM-plates (4000 cells/well) in serum-free medium and treated directly as described for the Alamarblue assay (3–6 replicates/treatment). The lower chambers were filled with (10%) FBS-supplemented medium used as a chemo attractant. Cell invasion was detected by electric sensors, measuring the impedance response, on the bottom of the upper chamber while the cells were penetrating the membrane. Real time measurements of cell migration/invasion were performed at 30 min intervals and the impedance responses were interpreted by the RTCA software and converted to cell indices. Statistics were performed using the Mann–Whitney U test.

Supplementary Material

Refer to Web version on PubMed Central for supplementary material.

Acknowledgments

The work was supported by the Swedish Cancer Society, The Swedish Research Council, BioCARE, Berta Kamprad Foundation, The Gunnar Nilsson Cancer Foundation, The Gustav Vth Jubilee Foundation, and Governmental Support for Medical Research (ALF). We thank Professor Lars Rönnstrand for providing us with PLX4032.

References

Bonazzi VF, Nancarrow DJ, Stark MS, et al. Cross-platform array screening identifies COL1A2, THBS1, TNFRSF10D and UCHL1 as genes frequently silenced by methylation in melanoma. PLoS One. 2011; 6:e26121. [PubMed: 22028813]

Chapman PB, Hauschild A, Robert C, et al. Improved survival with vemurafenib in melanoma with BRAF V600E mutation. N Engl J Med. 2011; 364:2507–2516. [PubMed: 21639808]

Cheli Y, Ohanna M, Ballotti R, et al. Fifteen-year quest for microphthalmia-associated transcription factor target genes. Pigment Cell Melanoma Res. 2010; 23:27–40. [PubMed: 19995375]

Conway K, Edmiston SN, Khondker ZS, et al. DNA-methylation profiling distinguishes malignant melanomas from benign nevi. Pigment Cell Melanoma Res. 2011; 24:352–360. [PubMed: 21375697]

Dahl C, Abildgaard C, Riber-Hansen R, et al. KIT Is a Frequent Target for Epigenetic Silencing in Cutaneous Melanoma. J Invest Dermatol. 2014

Davies H, Bignell GR, Cox C, et al. Mutations of the BRAF gene in human cancer. Nature. 2002; 417:949–954. [PubMed: 12068308]

Du J, Miller AJ, Widlund HR, et al. MLANA/MART1 and SILV/PMEL17/GP100 are transcriptionally regulated by MITF in melanocytes and melanoma. Am J Pathol. 2003; 163:333–343. [PubMed: 12819038]

Easwaran H, Johnstone SE, Van Neste L, et al. A DNA hypermethylation module for the stem/progenitor cell signature of cancer. Genome Res. 2012; 22:837–849. [PubMed: 22391556]

Ecsedi S, Hernandez-Vargas H, Lima SC, et al. DNA methylation characteristics of primary melanomas with distinct biological behaviour. PLoS One. 2014; 9:e96612. [PubMed: 24832207]

Furuta J, Nobeyama Y, Umebayashi Y, et al. Silencing of Peroxiredoxin 2 and aberrant methylation of 33 CpG islands in putative promoter regions in human malignant melanomas. Cancer Res. 2006; 66:6080–6086. [PubMed: 16778180]

Gao L, Smit MA, van den Oord JJ, et al. Genome-wide promoter methylation analysis identifies epigenetic silencing of MAPK13 in primary cutaneous melanoma. Pigment Cell Melanoma Res. 2013; 26:542–554. [PubMed: 23590314]

Gao L, van den Hurk K, Moerkerk PT, et al. Promoter CpG Island Hypermethylation in Dysplastic Nevus and Melanoma: CLDN11 as an Epigenetic Biomarker for Malignancy. J Invest Dermatol. 2014

Garraway LA, Widlund HR, Rubin MA, et al. Integrative genomic analyses identify MITF as a lineage survival oncogene amplified in malignant melanoma. Nature. 2005; 436:117–122. [PubMed: 16001072]

Haq R, Shoag J, Andreu-Perez P, et al. Oncogenic BRAF regulates oxidative metabolism via PGC1alpha and MITF. Cancer Cell. 2013; 23:302–315. [PubMed: 23477830]

Harbst K, Staaf J, Lauss M, et al. Molecular profiling reveals low- and high-grade forms of primary melanoma. Clin Cancer Res. 2012; 18:4026–4036. [PubMed: 22675174]

Hodis E, Watson IR, Kryukov GV, et al. A landscape of driver mutations in melanoma. Cell. 2012; 150:251–263. [PubMed: 22817889]

Huang da W, Sherman BT, Lempicki RA. Systematic and integrative analysis of large gene lists using DAVID bioinformatics resources. Nat Protoc. 2009; 4:44–57. [PubMed: 19131956]

Jonsson G, Busch C, Knappskog S, et al. Gene expression profiling-based identification of molecular subtypes in stage IV melanomas with different clinical outcome. Clin Cancer Res. 2010; 16:3356–3367. [PubMed: 20460471]

Jonsson G, Dahl C, Staaf JS, et al. Genomic profiling of malignant melanoma using tiling-resolution arrayCGH. Oncogene. 2007; 26:4738–4748. [PubMed: 17260012]

Koga Y, Pelizzola M, Cheng E, et al. Genome-wide screen of promoter methylation identifies novel markers in melanoma. Genome Res. 2009; 19:1462–1470. [PubMed: 19491193]

Konieczkowski DJ, Johannessen CM, Abudayyeh O, et al. A melanoma cell state distinction influences sensitivity to MAPK pathway inhibitors. Cancer Discov. 2014

Krauthammer M, Kong Y, Ha BH, et al. Exome sequencing identifies recurrent somatic RAC1 mutations in melanoma. Nat Genet. 2012; 44:1006–1014. [PubMed: 22842228]

Landan G, Cohen NM, Mukamel Z, et al. Epigenetic polymorphism and the stochastic formation of differentially methylated regions in normal and cancerous tissues. Nat Genet. 2012; 44:1207–1214. [PubMed: 23064413]

Lauss M, Aine M, Sjodahl G, et al. DNA methylation analyses of urothelial carcinoma reveal distinct epigenetic subtypes and an association between gene copy number and methylation status. Epigenetics. 2012; 7:858–867. [PubMed: 22705924]

Li JL, Mazar J, Zhong C, et al. Genome-wide methylated CpG island profiles of melanoma cells reveal a melanoma coregulation network. Sci Rep. 2013; 3:2962. [PubMed: 24129253]

Lian CG, Xu Y, Ceol C, et al. Loss of 5-hydroxymethylcytosine is an epigenetic hallmark of melanoma. Cell. 2012; 150:1135–1146. [PubMed: 22980977]

Mansky KC, Sankar U, Han J, et al. Microphthalmia transcription factor is a target of the p38 MAPK pathway in response to receptor activator of NF-kappa B ligand signaling. J Biol Chem. 2002; 277:11077–11083. [PubMed: 11792706]

Marzese DM, Scolyer RA, Huynh JL, et al. Epigenome-wide DNA methylation landscape of melanoma progression to brain metastasis reveals aberrations on homeobox D cluster associated with prognosis. Hum Mol Genet. 2013

Marzese DM, Scolyer RA, Roque M, et al. DNA methylation and gene deletion analysis of brain metastases in melanoma patients identifies mutually exclusive molecular alterations. Neuro Oncol. 2014; 16:1499–1509. [PubMed: 24968695]

Miller AJ, Levy C, Davis IJ, et al. Sumoylation of MITF and its related family members TFE3 and TFEB. J Biol Chem. 2005; 280:146–155. [PubMed: 15507434]

Murakami H, Arnheiter H. Sumoylation modulates transcriptional activity of MITF in a promoter-specific manner. Pigment Cell Res. 2005; 18:265–277. [PubMed: 16029420]

Noushmehr H, Weisenberger DJ, Diefes K, et al. Identification of a CpG island methylator phenotype that defines a distinct subgroup of glioma. Cancer Cell. 2010; 17:510–522. [PubMed: 20399149]

Sharma SV, Lee DY, Li B, et al. A chromatin-mediated reversible drug-tolerant state in cancer cell subpopulations. Cell. 2010; 141:69–80. [PubMed: 20371346]

Sigalotti L, Covre A, Fratta E, et al. Whole genome methylation profiles as independent markers of survival in stage IIIC melanoma patients. J Transl Med. 2012; 10:185. [PubMed: 22950745]

Steingrimsson E, Copeland NG, Jenkins NA. Melanocytes and the microphthalmia transcription factor network. Annu Rev Genet. 2004; 38:365–411. [PubMed: 15568981]

Tanemura A, Terando AM, Sim MS, et al. CpG island methylator phenotype predicts progression of malignant melanoma. Clin Cancer Res. 2009; 15:1801–1807. [PubMed: 19223509]

Thomas NE, Slater NA, Edmiston SN, et al. DNA methylation profiles in primary cutaneous melanomas are associated with clinically significant pathologic features. Pigment Cell Melanoma Res. 2014; 27:1097–1105. [PubMed: 24986547]

van den Hurk K, Niessen HE, Veeck J, et al. Genetics and epigenetics of cutaneous malignant melanoma: a concert out of tune. Biochim Biophys Acta. 2012; 1826:89–102. [PubMed: 22503822]

Vashisht Gopal YN, Rizos H, Chen G, et al. Inhibition of mTORC1/2 overcomes resistance to MAPK pathway inhibitors mediated by PGC1alpha and Oxidative Phosphorylation in melanoma. Cancer Res. 2014

Weisenberger DJ, Siegmund KD, Campan M, et al. CpG island methylator phenotype underlies sporadic microsatellite instability and is tightly associated with BRAF mutation in colorectal cancer. Nat Genet. 2006; 38:787–793. [PubMed: 16804544]

Wu M, Hemesath TJ, Takemoto CM, et al. c-Kit triggers dual phosphorylations, which couple activation and degradation of the essential melanocyte factor Mi. Genes Dev. 2000; 14:301–312. [PubMed: 10673502]

Yokoyama S, Woods SL, Boyle GM, et al. A novel recurrent mutation in MITF predisposes to familial and sporadic melanoma. Nature. 2011; 480:99–103. [PubMed: 22080950]

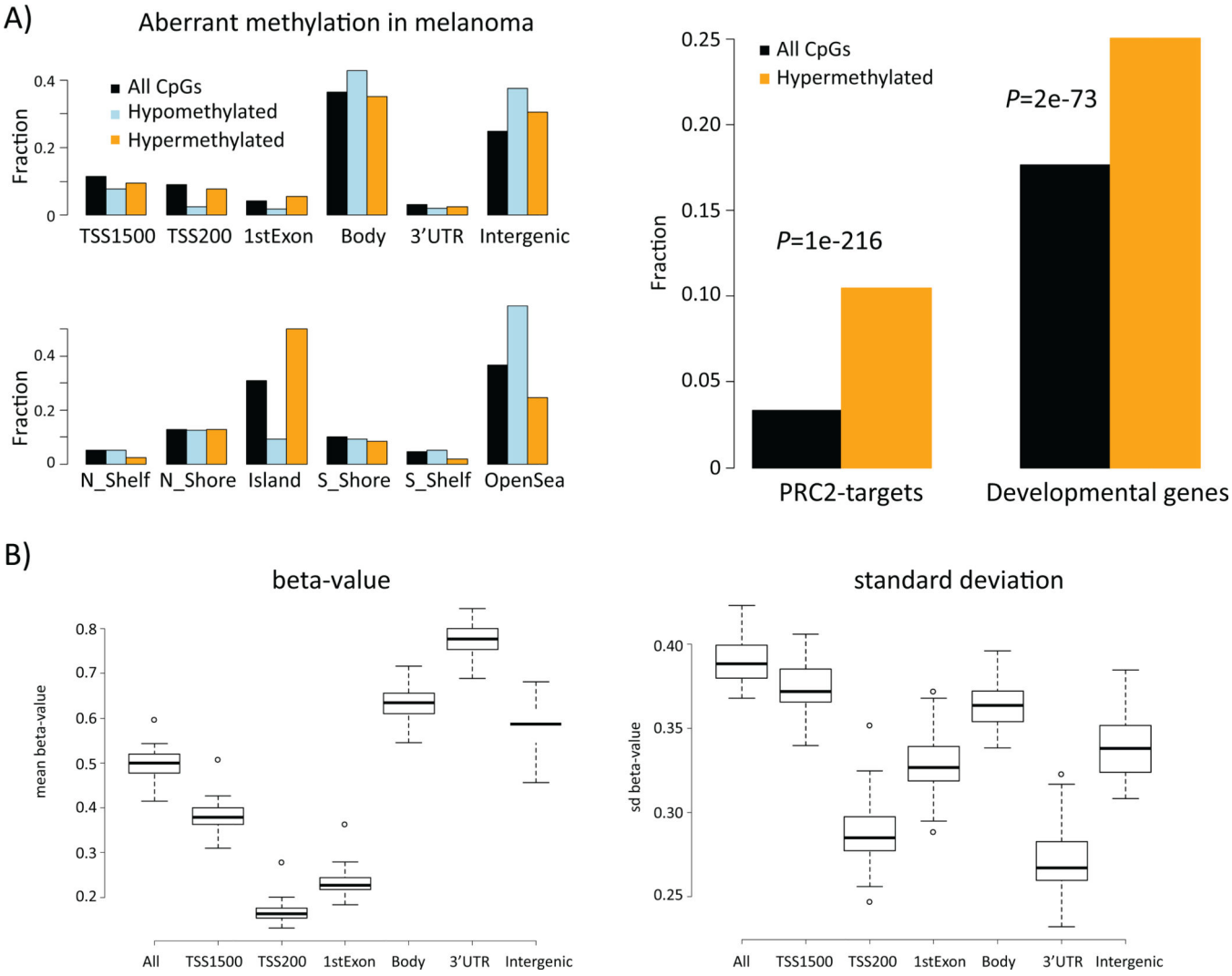

Figure 1.

DNA methylation patterns in melanoma. A) Location of hypomethylated and hypermethylated CpGs as well as all platform CpGs in respect to genes and CpG island annotations (left panel). Functional enrichment of genes that contain hypermethylated CpGs (right panel). For a given set of CpGs (all/hypo-meth./hyper-meth.) a bar indicates the fraction of CpGs assigned to the respective annotation. TSS1500 = 1500 to 201 bp upstream of transcription start, TSS200 = 200bp to transcription start site, Body = gene body. PRC2-targets = set of genes that is targeted by histone H3K27-methylating complex PRC2 (Lee et al., Cell 2006) B) DNA methylation characteristics across 50 melanomas; mean of β-values (left) and standard deviation of β-values (right) along the genes.

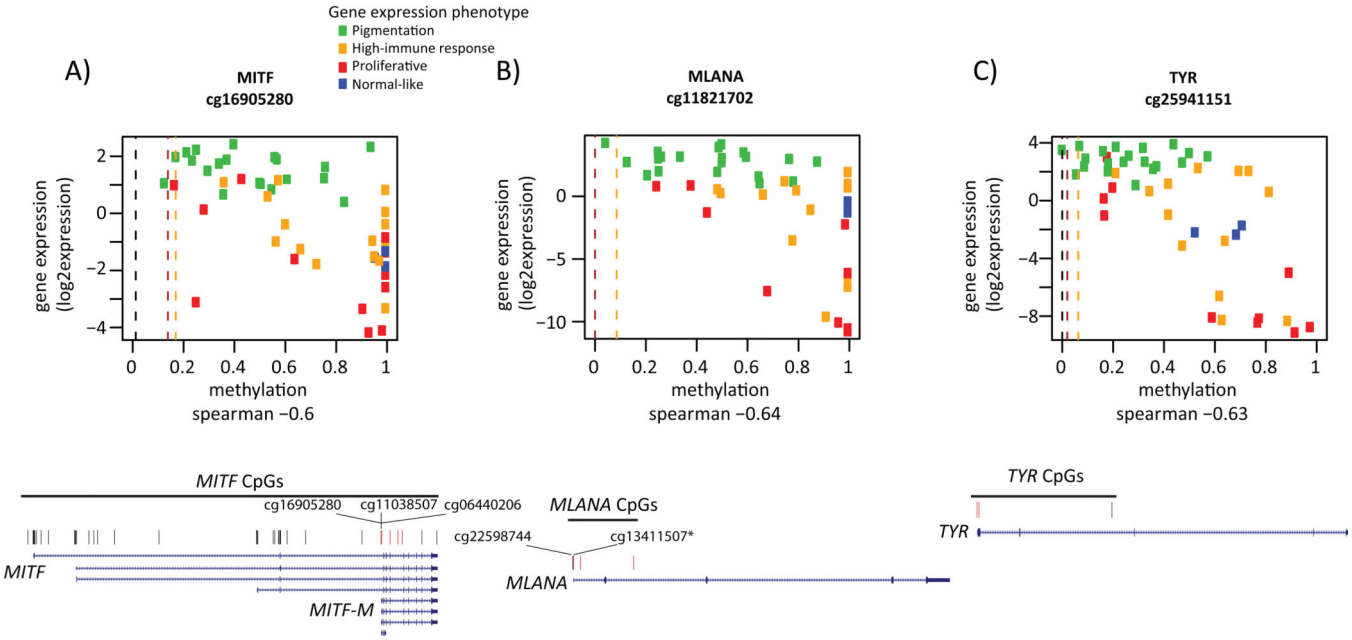

Figure 2.

Correlation of gene methylation status and gene expression levels in *MITF* and MITF targets. For the CpG with the largest negative correlation value in *MITF* (A), and its target genes *MLANA* (B) and *TYR* (C) β-values are plotted against gene expression values for the respective gene. In each plot, dots represent individual tumors and are colored according to gene expression phenotype. Methylation levels of light (orange), medium (dark red) and dark (brown) melanocytes are shown as dashed lines. Below each plot the gene structure and position of each measured CpG is shown. CpGs with significant correlation between methylation and gene expression are labeled red (an asterisk indicates one of the three significant CpGs in *MLANA*).

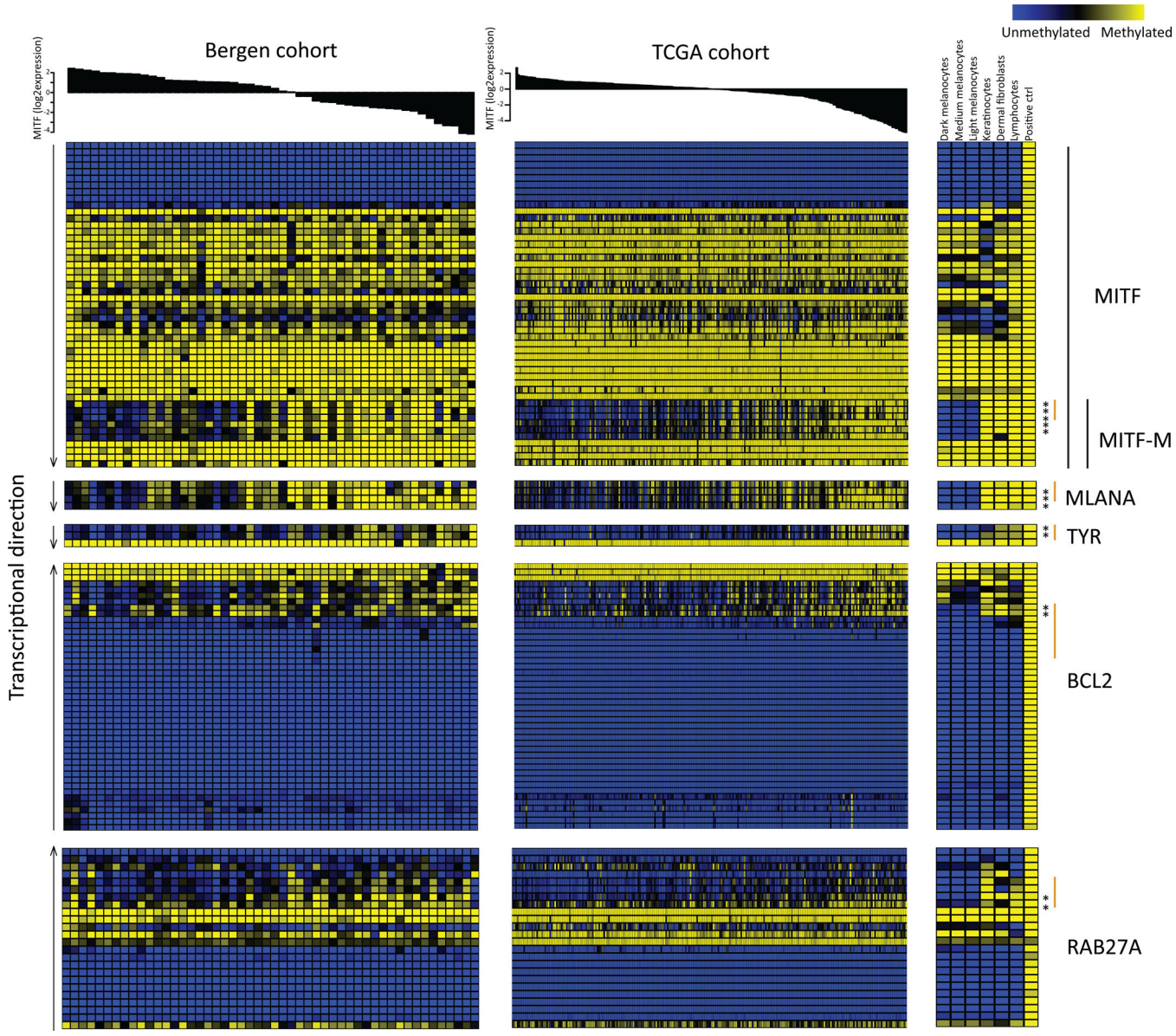

Figure 3.

DNA methylation status of *MITF* and MITF pathway genes. Tumors in the Bergen and TCGA cohorts are ordered according to *MITF* gene expression. *MITF* and selected MITF target genes are plotted and CpGs are ordered according to genomic position. An asterisk indicates CpGs with significant negative correlation between methylation and gene expression and TSS regions (+/− 1500bp from TSS) that include significant CpGs are marked by an orange line. The methylation status for normal cells is also shown.

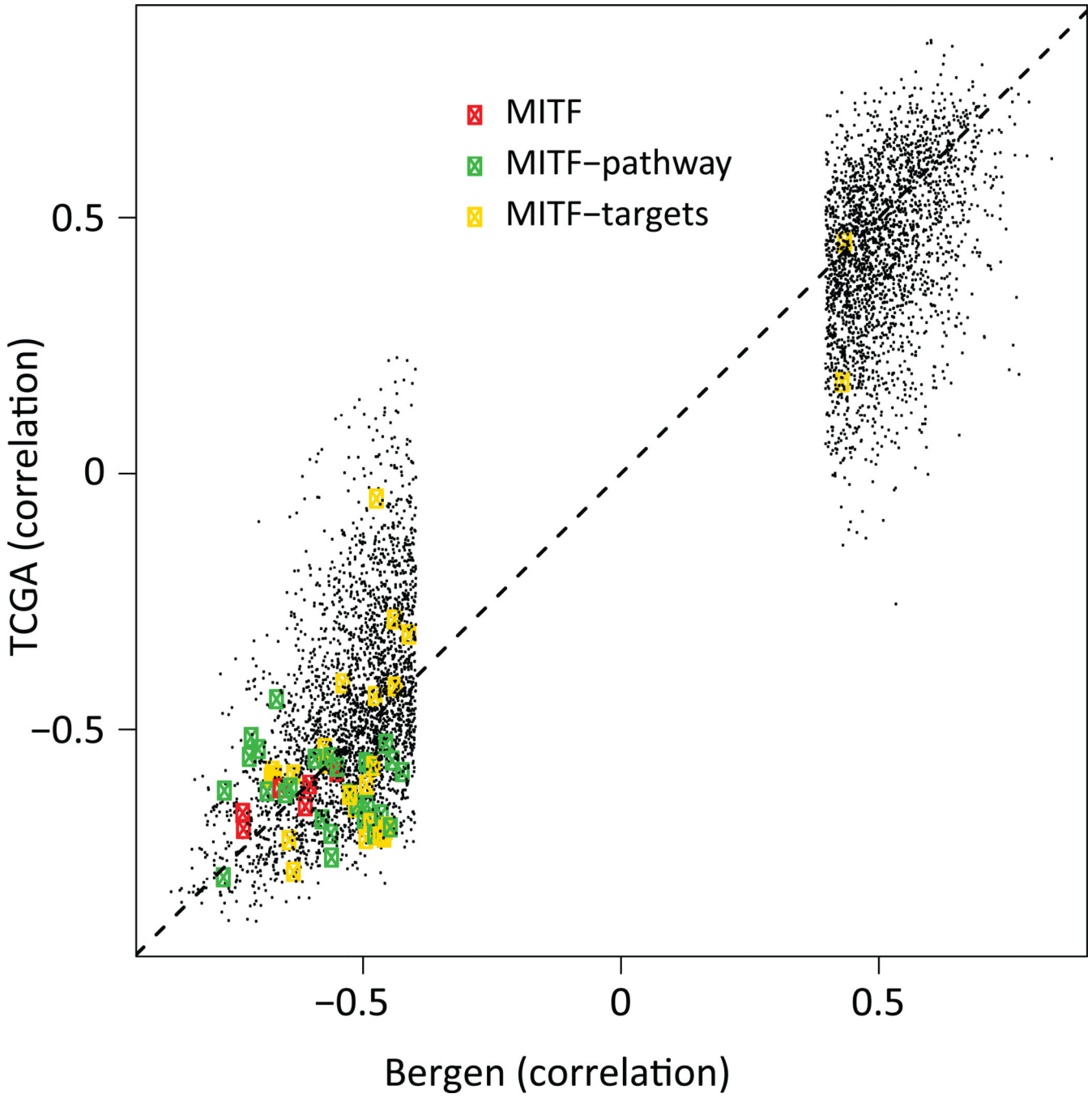

Figure 4.
Correlation of gene methylation status and gene expression levels in the Bergen and TCGA cohorts. Each dot represents a CpG's correlation to gene expression.

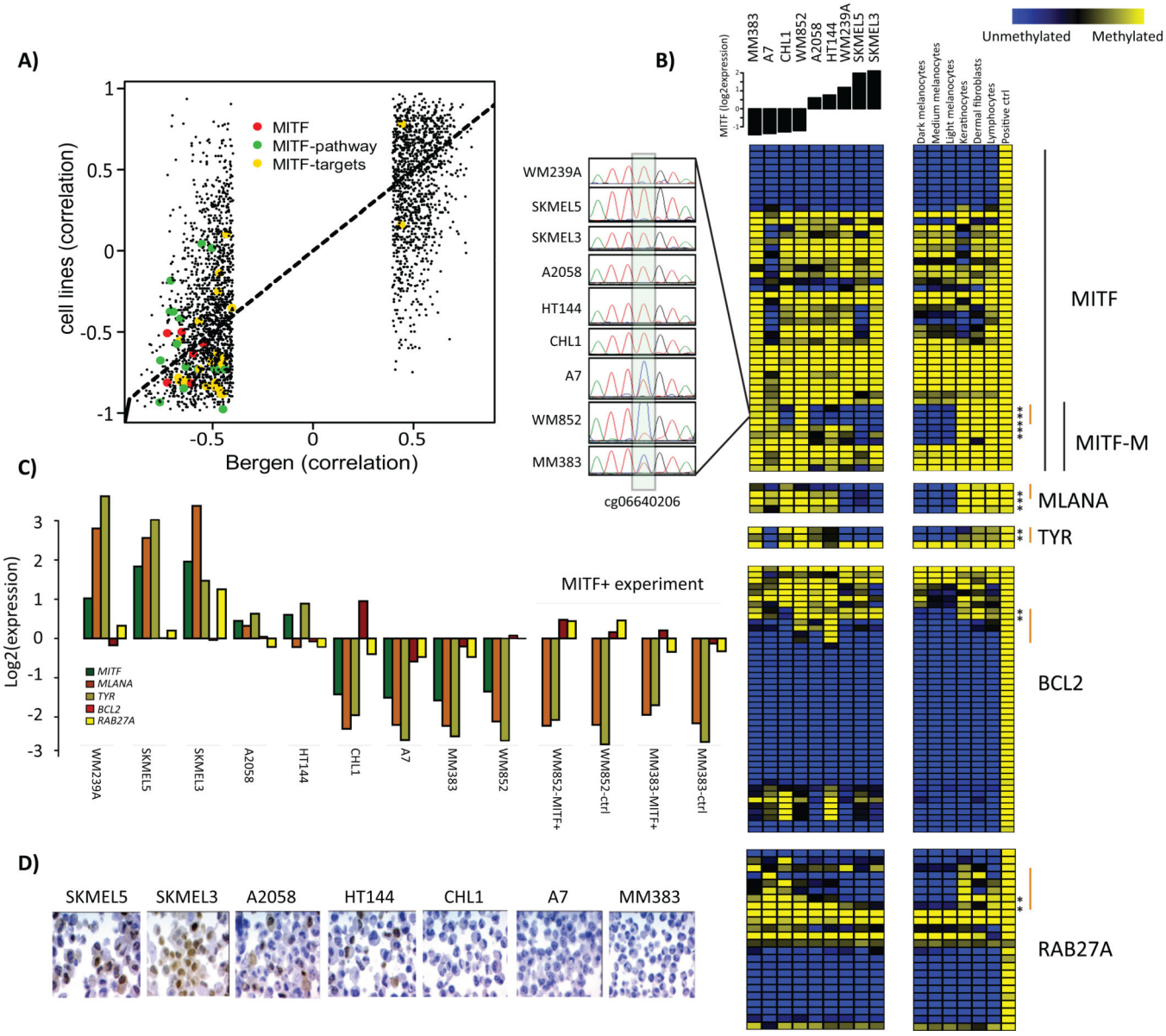

Figure 5.

MITF pathway methylation in melanoma cell lines. A) Correlation of gene methylation status and gene expression levels in the Bergen and cell line cohorts. Each dot represents a CpG's correlation to gene expression. B) DNA methylation status of CpGs covering the genes *MITF*, *MLANA*, *TYR*, *BCL2* and *RAB27A* across all melanoma cell lines and normal cells (melanocytes, keratinocytes, dermal fibroblasts and lymphocytes). CpGs are ordered according to genomic position. TSS regions (+/− 1500bp from TSS) that includes significant CpGs are marked by an orange line. Furthermore, the DNA methylation status of cg06640206 in the MITF-M TSS was fully validated using bisulfite Sanger sequencing. C) Microarray gene expression values for the selected MITF genes in all melanoma cell lines. Expression values are also shown for WM852 and MM383 cells overexpressing MITF. Notably, *MITF* gene expression was not measured since the probe on the array is located

outside of the MITF-M insert. D) MITF immunohistochemistry in melanoma cell lines with varying levels of *MITF*.

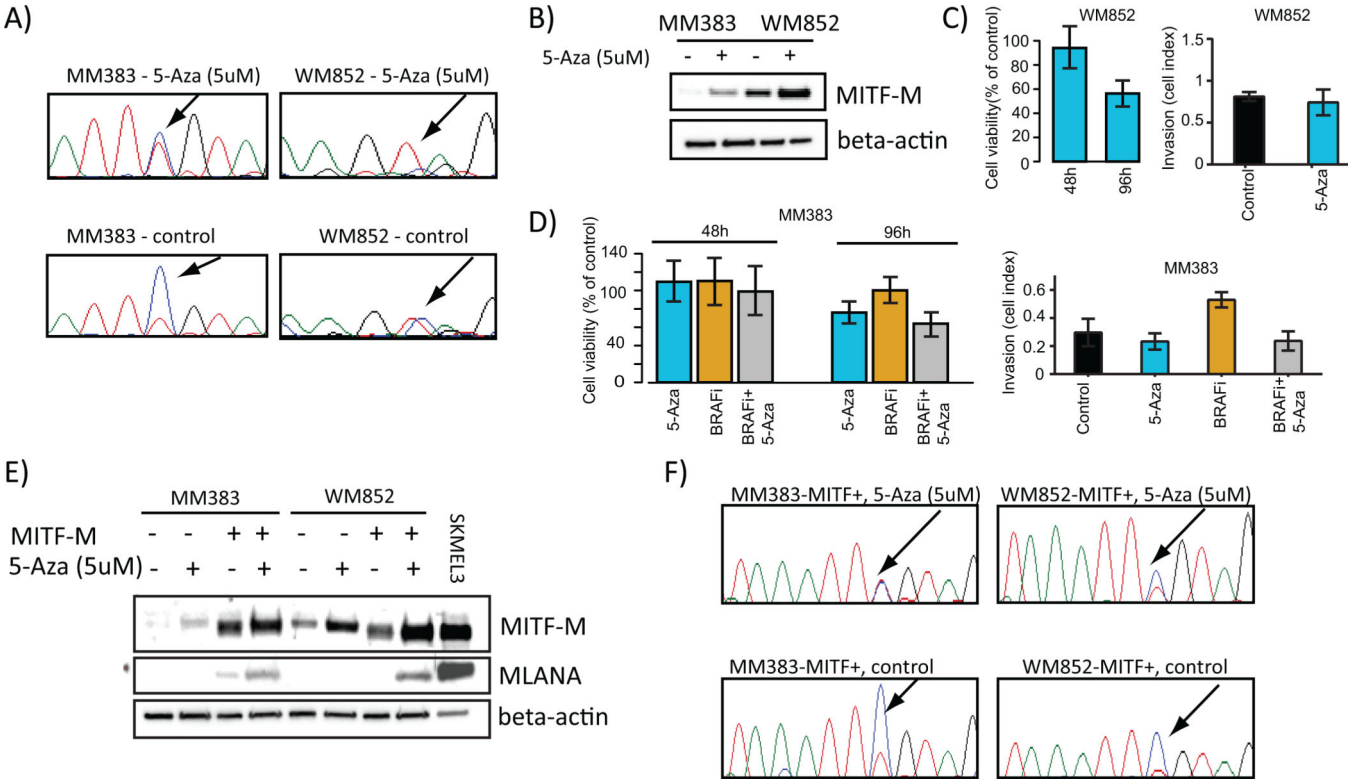

Figure 6.

MITF expression and activity is regulated by CpG methylation. A) Bisulphite Sanger sequencing confirms demethylation of the *MITF-M* promoter in MM383 and WM852 cells treated with 5uM 5-Aza. B) Western blot analysis of MITF-M following 5-Aza treatment for 96 hours in MM383 and WM852 cell lines. C) Proliferation and invasion assays showing 5-Aza effects on WM852 cells. Invasion assay was performed after 96 hours. D) Proliferation and invasion assays showing 5-Aza and BRAF inhibition (BRAFi) effects on MM383 cells. Left plot shows proliferative capacity of MM383 cells treated with 5-Aza, BRAFi or the combination. Right plot shows invasive capacity of MM383 cells treated with 5-Aza, BRAFi or the combination. E) Western blot analysis of MITF-M and MLANA following 5-Aza treatment for 96 hours in MM383 and WM852 cell lines with and without exogenous over expression of MITF-M. As a control, protein lysate from SKMEL3 was included. F) Bisulphite Sanger sequencing confirms demethylation of the *MITF-M* promoter in MM383-MITF-M+ and WM852-MITF-M+ cells treated with 5-Aza. Adenosine, green; cytosine, blue; guanine, black; thymidine, red.